High Performance Gigahertz Flexible Radio Frequency Transistors with Extreme Bending Conditions

Mengfei Wang[1,2], Mengchuan Tian[2], Zhenfeng Zhang[2], Shengman Li[1,2], Runsheng Wang[1], Chengru Gu[2], Xiaoyu Shan[2], Xiong Xiong[1,2], Xuefei Li[2], Ru Huang[1] and Yanqing Wu[1,2]*
[1]Institute of Microelectronics and Key Laboratory of Microelectronic Devices and Circuits (MoE), Peking University, Beijing 100871, *E-mail: yqwu@pku.edu.cn
[2]Wuhan National High Magnetic Field Center and School of Electrical and Electronic Engineering, Huazhong University of Science and Technology, Wuhan 430074, China,

Abstract— In this work, ultrathin indium tin oxide (ITO) radio frequency (RF) transistors have been demonstrated for the first time, where inverted gate structure are used with a flexible polyimide substrate using magnetron sputtering at a thermal budget below 200 ℃. The 160 nm channel length device exhibits excellent DC characteristics, including mobility of 26 $cm^2/V\cdot s$ and an I_{on}/I_{off} ratio of 6.6×10^8. A record-high extrinsic cut-off frequency (f_T) of 2.1 GHz and an extrinsic maximum oscillation frequency (f_{max}) of 3.7 GHz have also been obtained, which are more than one order of magnitude higher than previous results on flexible substrate. A high conversion gain of -20.9 dB has been achieved for the gigahertz frequency mixer based on flexible ITO RF transistor. Moreover, the stability of DC and RF performance under different bending conditions up to 50,000 bending cycles or down to 1 mm bending radius are studied without device failure.

I. Introduction

The application of flexible metal oxide TFTs in the high-frequency field has attracted more and more attention due to the advantages of metal oxides over amorphous silicon or organic semiconductors, such as high transparency, high mobility, and feasible fabrication process. However, the radio frequency performance of previous metal oxide TFT and other technologies are still unsatisfactory with cut off frequency typically in the MHz range. For example, the best extrinsic cut-off frequency (f_T) of flexible organic radio frequency (RF) transistors is only 6.7 MHz so far [1]. For the most common metal oxide, the maximum f_T of flexible IGZO RF transistors is only 135 MHz due to the low carrier mobility of about 10 $cm^2/V\cdot s$, which is far from the requirement for the internet of things (IoT) applications [2]. In contrast, ultrathin indium tin oxide thin-film transistors (ITO TFTs) exhibit higher mobility and excellent output characteristics, making ITO ideal material for flexible RF transistors or mixers operating at gigahertz regime. Moreover, bending stability is also critical for high-performance flexible RF electronics. Flexible ITO RF transistors could achieve excellent strain tolerance by depositing high-quality HfO_2 dielectric and interfaces with low trap density through atomic layer deposition (ALD) technique.

In this work, we have fabricated ITO RF transistors on flexible polyimide substrate using ALD and magnetron sputtering processes with maximum processing temperature of 200 ℃. Excellent DC and RF properties have been obtained, including high field-effect mobility (μ_{FE}), a high I_{on}/I_{off} ratio, an excellent f_T, and a high maximum oscillation frequency (f_{max}). Gigahertz Frequency mixer based on flexible ITO RF transistor has been demonstrated for the first time. All expected harmonics and a high conversion gain have been obtained. Moreover, the electrical performance variations of flexible ITO RF transistor under extreme bending conditions have been systematically investigated.

II. Device Structure and Fabrication

Fig. 1 shows the structure schematic of the flexible ITO RF transistor with two-finger inverted gate and ground-signal-ground (GSG) pad structure. The device was fabricated using standard fabrication processes, including electron beam lithography and e-beam evaporation. First, 125 µm thick polyimide substrate was sequentially sonicated in acetone, isopropanol, and water for 10 minutes to remove surface impurities and organics. Then, 100 nm thick SiN_x was deposited by PECVD to smooth the surface of the polyimide substrate. A stack of 20 nm thick Ni and 60 nm thick Au as the inverted gate was deposited by e-beam evaporation. Next, 10 nm thick HfO_2 as gate dielectric was deposited by ALD at 140°C using $Hf[N(CH_3)(C_2H_5)]_4$ and O_3. Subsequently, the ITO layer was deposited by magnetron sputtering at 200 ℃ with oxygen to argon ratio of 1 to 9. Finally, source and drain electrodes consisted of 20 nm thick Ni and 60 nm thick Au were patterned by electron beam lithography and deposited by e-beam evaporation. Throughout the whole fabrication process, the polyimide substrate was attached on the silicon chip with a PDMS film as the adhesion layer.

Fig. 2 shows the scanning electron microscopy (SEM) images of the flexible two-finger ITO RF transistor with a channel length of 160 nm and a channel width of 15 µm. The atomic force microscope (AFM) images in Fig. 3 show that the thickness of the ITO film is 5.6 nm, and the surface roughness root means square (RMS) is 0.37 nm. The oxygen-related chemical bond compositions in the ITO film were studied employing XPS-peak-differentiating analysis as shown in Fig. 4. The O 1s peak was divided into three peaks by Gaussian fitting with the elimination of a Shirley type background. Three

Authorized licensed use limited to: Huazhong University of Science and Technology. Downloaded on June 15,2020 at 03:26:15 UTC from IEEE Xplore. Restrictions apply.

peaks centered at 531.9 eV, 531 eV, and 529.6 eV, respectively, corresponding to oxygen impurities absorbed on the surface, oxygen-related defects, and oxygen bonded to metal. Oxygen vacancies account for 30% of all oxygen-related chemical bonds.

III. Results and Discussion

Fig. 5 and Fig. 6 show the transfer and output characteristics of the flexible ITO RF transistor, respectively. The inset is the optical image of a flexible sample clamped between fingers. Typical characteristics were achieved including an I_{on}/I_{off} ratio of 6.6×10^8, a threshold voltage (V_{th}) of 1.15 V, a μ_{FE} of 26 $cm^2/V\cdot s$, a sub-threshold slope (SS) of 120 mV/decade, a maximum drain current (I_{dmax}) of 83.2 μA/μm, and an on-resistance (R_{on}) of 14.4 Ω·mm.

Standard S-parameter measurements were carried out to evaluate the high-frequency properties of the flexible ITO RF transistor. Fig. 7 shows the small-signal current gain ($|h_{21}|$) and unilateral power gain (U) as a function of frequency for the device with a channel length of 160 nm. The extrinsic f_T of 2.1 GHz was obtained, which is the highest value among flexible metal oxide or organic RF transistors as shown in Fig. 8, more than 10 times larger than the previous best results [1-5]. Also, the extrinsic f_{max} of 3.7 GHz is the highest value achieved on flexible metal oxide transistors so far. Fig. 9 shows that the voltage gain (Z_{21}/Z_{11}) extracted from the S-parameters remains positive until the frequency reaches 3 GHz.

The electrical performance of frequency mixer based on flexible ITO RF transistor has been investigated for the first time. The measurement setup for flexible ITO mixer is shown in Fig. 10, where the gate mixing of the local oscillator (LO) and RF signals with an external power combiner was used. Fig. 11 shows the output frequency spectrum of the flexible ITO mixer with f_{RF} = 1.5 GHz, P_{RF} = 12 dBm and f_{LO} = 1.4 GHz, P_{LO} = 0 dBm. A distinct immediate frequency f_{IF} = 100 MHz together with other expected harmonics were obtained. The conversion gain versus input power at different input LO power with f_{RF} = 1.5 GHz and f_{LO} = 1.4 GHz is shown in Fig. 12. As the LO power increases, the conversion gain gradually increases to a high value of -20.9 dB and 1dB compression point (CP_{1dB}) remains constant at 1.7dBm.

The bending effects on the DC and RF characteristics of flexible ITO RF transistor have been investigated using a custom-built bending apparatus. Fig. 13 shows the transfer characteristics as a function of the bending cycle from 0 to 50,000, which is the largest bending cycle among flexible RF transistors. The bending radius is fixed at 10 mm, corresponding to a tensile strain of 0.63%. The dependence of typical characteristics including, V_{th}, normalized I_{dmax}, and normalized R_{on} on the bending cycle was extracted in Fig. 14 and Fig. 15. When the bending cycle changes from 0 to 50,000, V_{th} shifts negatively, I_{dmax} reduce to 54% of the original value, and R_{on} increases to 1.5 times the original value. Fig. 16 and Fig. 17 show the dependence of $|h_{21}|$ and U on the frequency at different bending cycles, respectively. As the bending cycle increases from 0 to 50,000, the curves shift negatively, correspondingly, the extrinsic f_T and extrinsic f_{max} regularly degrade for 36% and 32 %, respectively, as shown in Fig. 18.

Fig. 19 shows the transfer characteristics as a function of bending radius with a bending cycle of 1000. The bending radius starts at flat and then changes from 10 mm to 1 mm with a step of 1 mm, corresponding to a tensile strain of 0% and 0.63% to 6.24%, which is the highest tensile strain among flexible metal oxide RF transistors. The Excessive tensile strain would irreversibly crack all layers and interfaces of the device, thus worsen the electrical performance. As the tensile strain increases from 0 to 6.24%, transfer characteristic and V_{th} gradually shift negatively, correspondingly, I_{dmax} and R_{on} regularly deteriorate to 63%, and 215% of the initial value, as shown in Fig. 20 and Fig. 21. In Fig. 22 and Fig. 23, the variations of $|h_{21}|$ and U at different bending radius were measured under the same bending condition as Fig. 19. And the dependence of normalized f_T and normalized f_{max} on frequency was plotted in Fig. 24. With the tensile strain increasing to 6.24%, $|h_{21}|$ and U shift negatively as predicted. The extrinsic f_T and extrinsic f_{max} monotonically decrease by 51% and 43%, respectively. After these bending test, the flexible ITO RF transistor still works well and exhibits decent DC and RF characteristics even under extremely harsh bending conditions such as bending for 50,000 cycles at a radius of 10 mm or bending at a radius of 1 mm for 1000 cycles. The excellent bending stability of the device can be attributed to the high quality of ALD HfO_2 dielectric, ultrathin ITO channel, and the excellent interface.

IV. Conclusions

In summary, high-frequency ITO RF transistors have been fabricated on the flexible polyimide substrate. Due to the excellent transfer and output characteristics, a record-high extrinsic f_T of 2.1 GHz and an extrinsic f_{max} of 3.7 GHz have been achieved for the device with a channel length of 160 nm. Gigahertz ITO mixer on the flexible substrate has been constructed and a high conversion gain of -20.9 dB has been obtained. The excellent stability of DC and RF performance under extremely harsh bending conditions has been systematically studied without device failure. These results indicate the remarkable potential of flexible ITO RF transistors for high-frequency applications.

Acknowledgment

This work was supported by the Natural Science Foundation of China (Grant Nos. 61574066, 61874162 and 61421005) and 111 Project (B18001).

References

[1] Borchert, J. et al., in *2018 IEEE International Electron Devices Meeting (IEDM)* 38.4.1-38.4.4 (2018).
[2] Münzenrieder, N. et al., *IEEE Trans. Electron Devices* 60, 2815-2820 (2013).
[3] Münzenrieder, N. et al., in *2012 International Electron Devices Meeting*, 5.2.1-5.2.4 (2012).
[4] Carta C. et al., in *2013 SBMO/IEEE MTT-S International Microwave & Optoelectronics Conference (IMOC)*, 1-2 (2013).
[5] Münzenrieder N. et al., *IEEE Electron Device Lett.* 35, 69-71 (2014).

Authorized licensed use limited to: Huazhong University of Science and Technology. Downloaded on June 15,2020 at 03:26:15 UTC from IEEE Xplore. Restrictions apply.

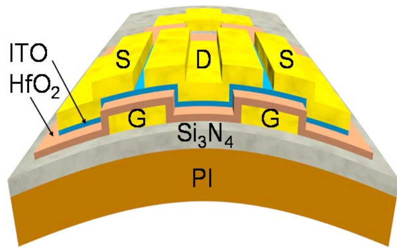

Fig. 1. Structure schematic of the flexible ITO RF transistor with dual-finger bottom gate structure. The thickness of HfO_2 and ITO is 10 nm and 5.6 nm, respectively.

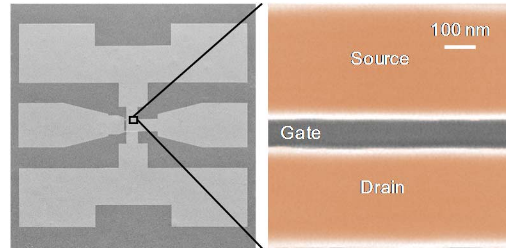

Fig. 2. Left: The SEM image of the flexible ITO RF transistor. Right: The SEM image of the channel with a length of 160 nm and a gate-source/drain overlap length of 300 nm. The scale bar is 100 nm.

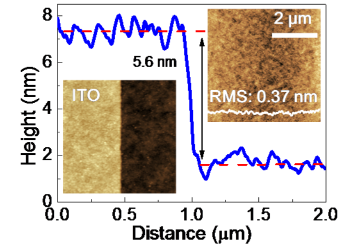

Fig. 3. The AFM images of the ITO boundary and surface. The scale bar is 2 μm.

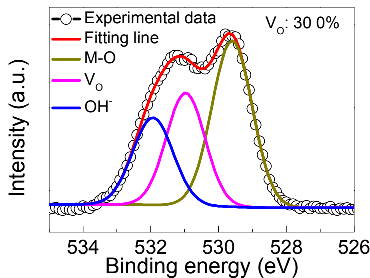

Fig. 4. The XPS spectra of the ITO film in O 1s region. The O 1s peak was divided into three peaks by Gaussian fitting.

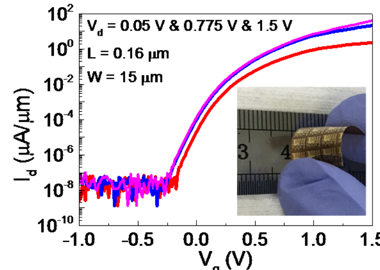

Fig. 5. Transfer characteristic of the flexible ITO RF transistor. The inset is the optical image of a flexible ITO RF sample.

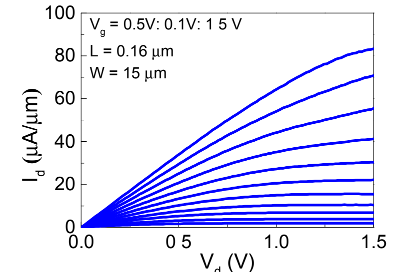

Fig. 6. Output characteristic of the flexible ITO RF transistor.

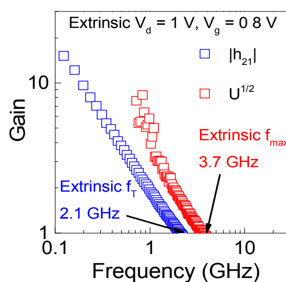

Fig. 7. Small-signal current gain ($|h_{21}|$) and unilateral power gain (U) versus frequency for the flexible ITO RF transistor at V_d = 1 V and V_g = 0.8 V.

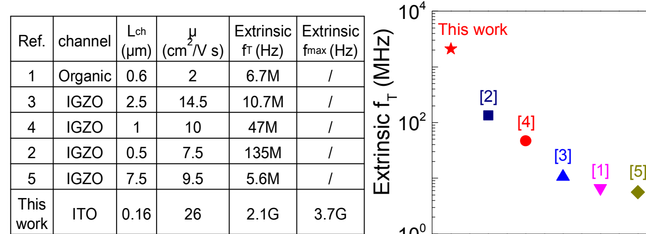

Ref.	channel	L_{ch} (μm)	μ (cm^2/V s)	Extrinsic f_T (Hz)	Extrinsic f_{max} (Hz)
1	Organic	0.6	2	6.7M	/
3	IGZO	2.5	14.5	10.7M	/
4	IGZO	1	10	47M	/
2	IGZO	0.5	7.5	135M	/
5	IGZO	7.5	9.5	5.6M	/
This work	ITO	0.16	26	2.1G	3.7G

Fig. 8. Left: Benchmark of high-frequency performance of this work with flexible organic or metal oxide RF transistors in literature. Right: Benchmark of extrinsic f_T among flexible metal oxide or organic RF transistors.

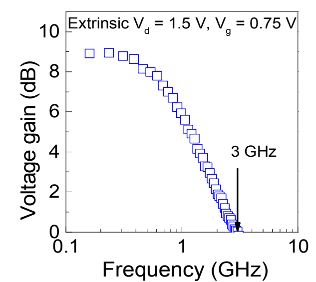

Fig. 9. Voltage gain (Z_{21}/Z_{11}) versus frequency for the flexible ITO RF transistor at V_d = 1.5 V and V_g = 0.75 V.

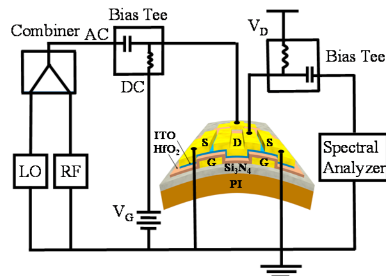

Fig. 10. Measurement setup for flexible ITO mixer.

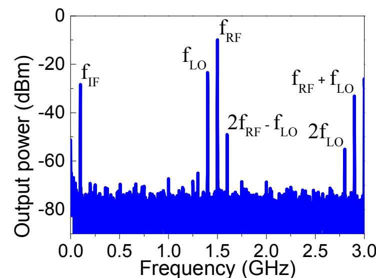

Fig. 11. Output frequency spectrum of the flexible ITO mixer with f_{RF} = 1.5 GHz, P_{RF} = 12 dBm and f_{LO} = 1.4 GHz, P_{LO} = 0 dBm.

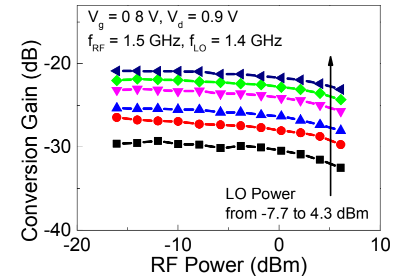

Fig. 12. Conversion gain versus input RF power at different input LO power for the flexible ITO mixer. V_g = 0.8 V, V_d = 0.9 V, and f_{RF} = 1.5 GHz, f_{LO} = 1.4 GHz. P_{LO} = -7.7 dBm, -4.7 dBm, -2.7 dBm, 0.3 dBm, 2.3 dBm, 4.3 dBm.

Authorized licensed use limited to: Huazhong University of Science and Technology. Downloaded on June 15,2020 at 03:26:15 UTC from IEEE Xplore. Restrictions apply.

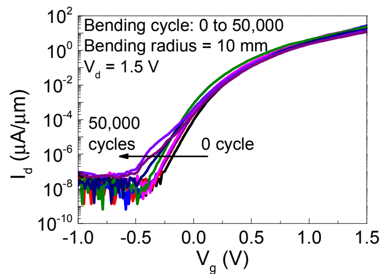

Fig. 13. Transfer characteristics as a function of bending cycle from 0 to 50,000 at a bending radius of 10 mm for flexible ITO RF transistor at V_d = 1.5 V.

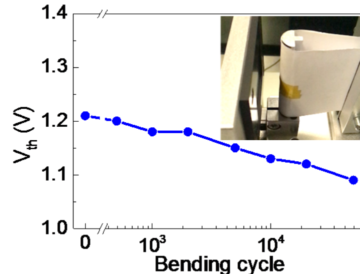

Fig. 14. Dependence of threshold voltage (V_{th}) on the bending cycle. The inset is the partial view of the bending apparatus.

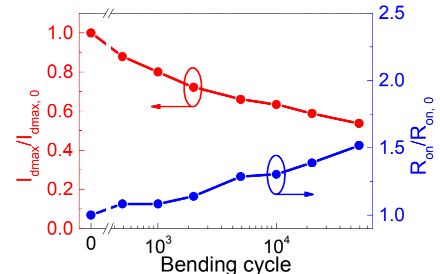

Fig. 15. Dependence of normalized maximum drain current (I_{dmax}) and normalized on-resistance (R_{on}) on the bending cycle.

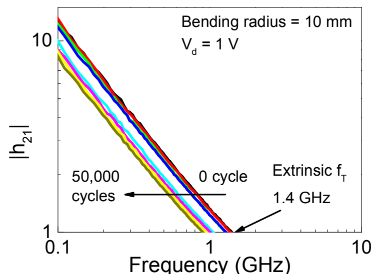

Fig. 16. Small-signal current gain ($|h_{21}|$) versus frequency at different bending cycles. Bending radius = 10 mm and V_d = 1 V.

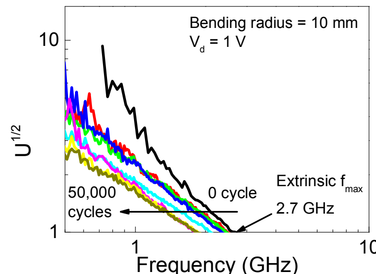

Fig. 17. Unilateral power gain (U) versus frequency at different bending cycles. Bending radius = 10 mm and V_d = 1 V.

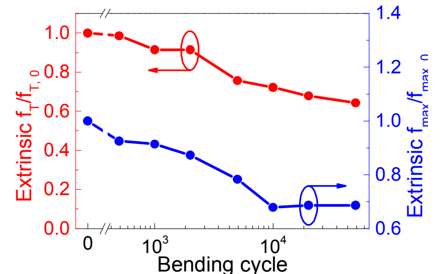

Fig. 18. Dependence of normalized extrinsic cut-off frequency (f_T) and normalized extrinsic maximum oscillation frequency (f_{max}) on the bending cycle.

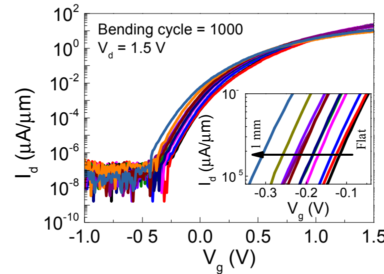

Fig. 19. Transfer characteristics as a function of bending radius from 10 mm to 1 mm at a bending cycle of 1000 for the flexible ITO RF transistor. V_d = 1.5 V.

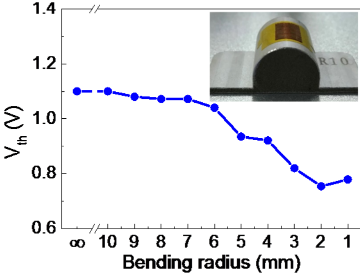

Fig. 20. Dependence of threshold voltage (V_{th}) on the bending radius. The inset is the flexible ITO RF sample attached to a cylinder.

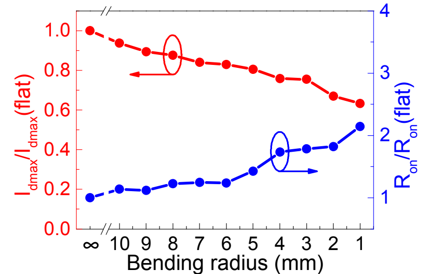

Fig. 21. Dependence of normalized maximum drain current (I_{dmax}) and normalized on-resistance (R_{on}) on the bending radius.

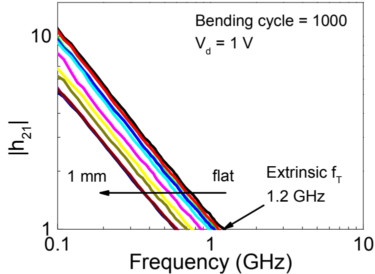

Fig. 22. Small-signal current gain ($|h_{21}|$) versus frequency at different bending radii. Bending cycle = 1000 and V_d = 1 V.

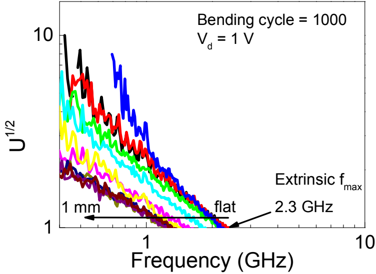

Fig. 23. Unilateral power gain (U) versus frequency at different bending radii. Bending cycle = 1000 and V_d = 1 V.

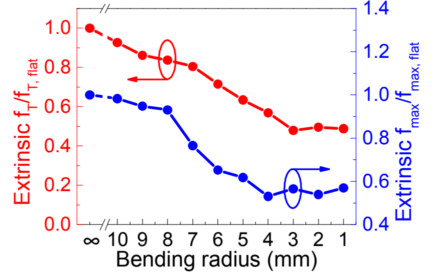

Fig. 24. Dependence of normalized extrinsic cut-off frequency (f_T) and normalized extrinsic maximum oscillation frequency (f_{max}) on the bending radius.

Authorized licensed use limited to: Huazhong University of Science and Technology. Downloaded on June 15,2020 at 03:26:15 UTC from IEEE Xplore. Restrictions apply.